C. R. Physique 20 (2019) 725–745

Contents lists available at ScienceDirect

Comptes Rendus Physique

www.sciencedirect.com

Science in the making 2: From 1940 to the early 1980s / *La science en mouvement 2 : de 1940 aux premières années 1980*

André Guinier: Local order in condensed matter

André Guinier : ordre local en matière condensée

Jean-Paul Pouget *, Anne-Marie Levelut, Jean-François Sadoc

Laboratoire de physique des solides, CNRS UMR 8502, Université Paris-Sud, Université Paris-Saclay, 91405 Orsay, France

ARTICLE INFO

Article history:
Available online 9 April 2019

Keywords:
History of crystallography
X-ray diffraction
Local order
Small-angle scattering
X-ray diffuse scattering

Mots-clés :
Histoire de la cristallographie
Diffraction des rayons X
Ordre local
Diffusion aux petits angles
Diffusion diffuse des rayons X

ABSTRACT

This contribution is a tribute to André Guinier and to the scientific school he created. We show how his thesis work allowed one to develop new X-ray scattering techniques of investigation of matter both at small and large scattering Bragg angles. In parallel to his pioneering experimental work, André Guinier introduced a well-adapted formalism allowing a precise characterization of various types of local order in the matter. These findings, which have been extended by his own students, have seed an "X-ray scattering" school of international reputation, which remains very active today. Here, we cover in detail the birth of this school from 1940 to 1980. Then, we outline the evolution of researches of the team he founded at the "Laboratoire de physique des solides" of Paris-Sud University until the beginning of the 21st century, when investigations using synchrotron radiation have revolutionized the study of the structure of the matter.

RÉSUMÉ

Cette contribution est un hommage à André Guinier et à l'école scientifique qu'il a créée. Nous montrons comment son travail de thèse a permis de développer de nouvelles méthodes d'étude de la matière par diffusion des rayons X aux petits et grands angles de Bragg. En parallèle à ce travail expérimental novateur, André Guinier a introduit un formalisme adapté, permettant une caractérisation précise de divers types d'ordre local dans la matière. Ces travaux, qui ont été étendus par ses propres étudiants, sont à l'origine d'une école de « diffraction des rayons X » de réputation internationale, qui reste très active de nos jours. Dans cet article, nous couvrons en détail la naissance de cette école de 1940 à 1980, puis nous survolons l'évolution des recherches de l'équipe qu'il a fondée au Laboratoire de physique des solides d'Orsay jusqu'au début du XXI^{e} siècle, lorsque les investigations par rayonnement synchrotron ont révolutionné l'étude de la structure de la matière.

---

* Corresponding author.
E-mail address: jean-paul.pouget@u-psud.fr (J.-P. Pouget).

https://doi.org/10.1016/j.crhy.2019.03.005

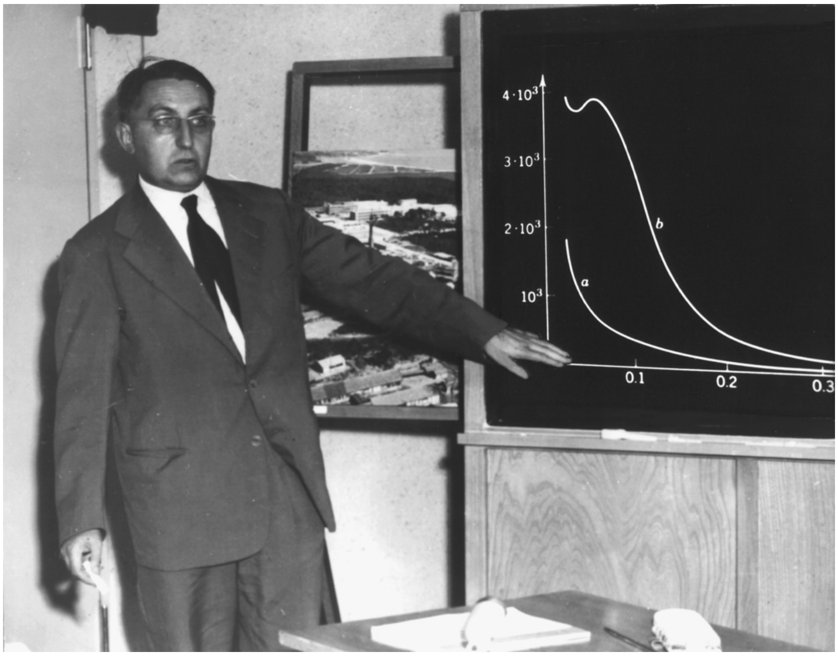

Fig. 1. André Guinier giving a lecture in Building 210 of the new Orsay campus in the 1960s. Classical SAXS spectra, where the diffracted intensity increases with decreasing θ, are drawn on the blackboard.

A major achievement of experimental research in the 19th century was the discovery of X-rays by Röntgen in 1895. With a wavelength (λ) of the order of 10^{-1} nm, comparable to interatomic distances in solid (or more especially to inter-planar distances d in crystals), it was demonstrated in 1912 by W. Friederich and P. Knipping, following a suggestion of M. von Laue, that an X-ray beam can strongly interact with matter. More precisely, interaction of an incoming X-ray beam with a crystal delimits a discrete set of outcoming beams forming a lattice of sharp reflections that can be indexed by periodic wave vectors ($\mathbf{G}$) of the so-called reciprocal space of the crystal. Furthermore, these scattered beams can be detected as intense spots on a photographic plate, forming a so-called Laue diagram when an incoming polychromatic X-ray beam is used. This scattering process, formalized by W.L. Bragg in 1913, allows one to determine inter-planar distances d between crystalline atomic layers according to the so-called Bragg law:

$$n\lambda = 2d\sin\theta,$$

where n is an integer and 2θ is the angle between the incoming and outcoming beams (defined in Fig. 2a). This simple relationship had a considerable output since it opens a new area of research, named crystallography, allowing one to determine atomic (molecular) arrangements in crystals, materials, minerals and "living" substances, object of numerous fields of research such as solid-state physics, metallurgy, chemistry, geology, and biology.

Soon it was realized that any kind of crystal imperfection (stacking defects, chemical disorder, lattice vibrations...) perturbing the long-range crystalline order probed by diffraction limits the intensity of Bragg reflections by a large attenuation factor. This loss of intensity is, however, recovered under the form of a very weak and broad diffuse background spread all over the reciprocal space between the set of sharp Bragg reflections. This broad X-ray scattering in $\mathbf{G}+\mathbf{q}$ is called diffuse scattering by opposition with the sharp Bragg scattering (or Bragg diffraction) located at reciprocal lattice positions $\mathbf{G}$. The originality of the scientific work of André Guinier (1911–2000) (Fig. 1; for a recent bibliography, see [1]) and his students was to set suitable experimental conditions allowing the detection of such a weak scattering both at small (let us say, a few degrees for a typical incoming X-ray beam) and large Bragg diffraction angles 2θ (small-angle X-ray scattering, SAXS, and wide-angle X-ray scattering, WAXS, respectively) and to develop the convenient formalism to analyze this scattering. In most of the cases, such a scattering reveals the presence of a local short-range atomic order, different than the long-range periodic order of crystals, which strongly influences the physical and chemical properties of materials.

This paper focuses on the main research directions developed by André Guinier during his scientific life and whose genesis can be found in his thesis work [2]. These researches were amplified by different generations of students, first at the "Conservatoire des arts et métiers" (CNAM) since 1940, then after 1959 at the "Laboratoire de physique des solides" (LPS), which he founded with Jacques Friedel and Raymond Castaing on the campus of Orsay (André Guinier was the first dean of this new faculty of science from 1958 to 1962). The creation of the LPS was an unprecedented occasion to mix together, in the same building, complementary fields of research that were in the 1960s separated in different laboratories: from

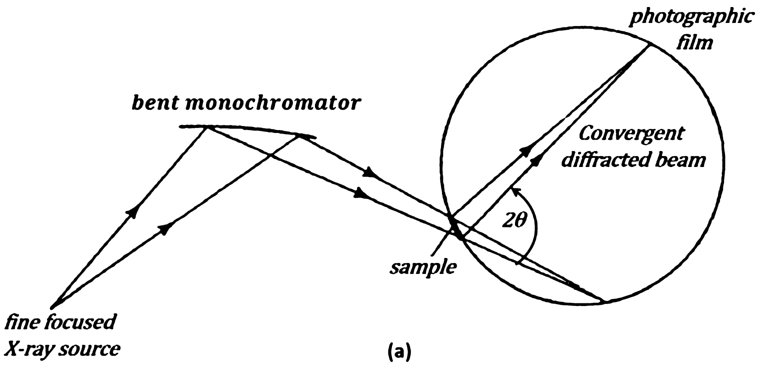

Fig. 2a. Principle of Guinier's camera.

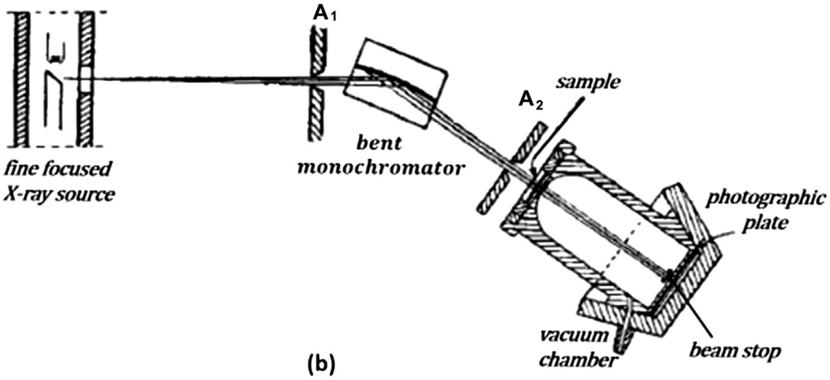

Fig. 2b. Prototype SAXS set-up built by André Guinier.

the organization of matter to its electronic/magnetic properties and from innovative scientific instrumentation to elaborated theory.

André Guinier's contribution in condensed matter can be classified as that of a crystallographer of what is not a perfect crystal. It is important to notice that this contribution cannot be apprehended without considering the broad scientific culture that was, and still is at the LPS, the interweaving between approaches based on a plurality of concepts often decoupled in other research centers. This was the case with metallurgy, the study of structural defects, but also of electronic and magnetic structures and, from the 1970s, of soft matter. Each domain then benefits from concepts developed in other disciplines, as it will be illustrated below.

1. The genesis of "out-of-Bragg reflection" crystallography

The context in which André Guinier developed his first scientific works is well summarized by himself in ref. [3]. The instrumentation developed during his thesis uses a focused monochromatic radiation issued from a fine focused X-ray source to obtain an intense diffraction pattern above a very small parasitic background (Fig. 2a). The set-up allowing one to study crystalline powders, which uses a bent quartz monochromator focusing scattered beams on a photographic film, and which incorporates a vacuum chamber to suppress air scattering, is referred to as a "Guinier camera" [4]. All experimental set-ups developed later for the study of X-ray diffuse scattering were derived from this principle. However, the realization of experiments becomes quite elaborate when cumbersome sample environments, such as furnace, cryostat (Fig. 2c) or pressure cell, have to be incorporated in the scattering path with the constraint to keep a low parasitic background.

Following the development of the "Guinier camera," SAXS apparatuses were built on the same principle (Fig. 2b). Low-θ SAXS experiments performed in conditions free from air contamination were able to reveal an intense X-ray scattering, increasing rapidly with decreasing θ (right part of Fig. 1) in diverse inhomogeneous materials and materials including fine particles such as charcoal, cellulose fibers, colloids, ovalbumin, and even in solutions of hemoglobin. The increase of the scattered intensity from dispersed particles (when the distance between particles is much larger than the particles'

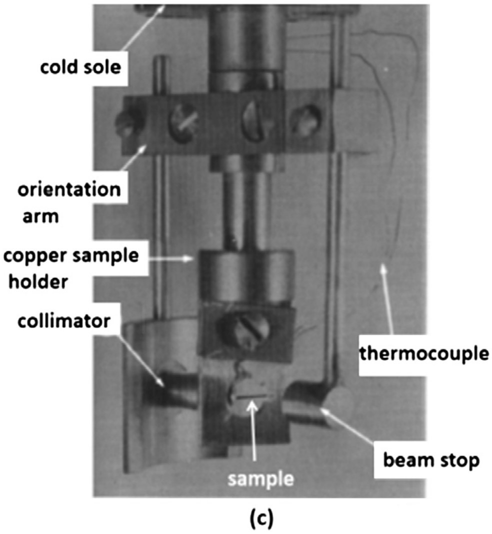

Fig. 2c. Sample-holder assembly developed at the end of the 1970s for low-temperature WAXS "monochromatic Laue" experiments, schematized in Fig. 4a. This assembly is attached to the cold sole of a cryocooler achieving regulated temperature from 10 to 300 K and placed inside an inner helium-filled can insuring thermalization of the sample. The cylindrical photographic film is fixed to an outer beryllium can. Vacuum is realized between the inner and outer cans.

dimension) was simply explained by the famous "Guinier law," allowing the determination of an "average size" of the particles investigated (called gyration radius[1] by Guinier), typically from 1 to 100 nm [5].

A remarkable discovery from SAXS studies of age-hardened Al–5%Cu alloys was the observation at low θ of a diffuse scattering in streaks corresponding to the segregation of Cu atoms in nanometric platelets [6,7]. This observation was also simultaneously and independently done by George Dawson Preston [7,8]. This discovery of the structural basis of the hardening effect has a considerable importance for metallurgical properties. This atomic segregation effect, found in many alloys and even in non-metallic crystals, is now explained in the literature as due to the formation of Guinier–Preston (GP) zones. The history of this important discovery is reported in refs. [9–11].

At this stage, it is important to mention how prolific and innovative was the thesis work of André Guinier performed just before the Second World War: Guinier's first camera in 1937, first article on SAXS in 1938, discovery of GP zones in 1938, and the defense of his thesis in 1939. These important discoveries have influenced his scientific approach throughout his career. Metallurgy, structural defects, order and disorder beyond classical crystallography became the dominant motivations of his future researches.

After the Second World War, SAXS experiments were further developed at CNAM during the thesis work of Gérard Fournet conducted under the supervision of André Guinier [12]. SAXS studies of GP zones were also completed by WAXS studies in Al–Ag [13,14] and Al–Cu (see figure XIII 44 in ref. [15]) single crystals.

André Guinier has also provided the principle of the electron microprobe to Raymond Castaing for his thesis research [16]. His thesis work, defended in 1951, had an important outcome with the development of electron microprobes for the study of matter. This aspect will be covered by Christian Colliex in this issue.

Another important contribution of André Guinier during this period was the writing of two textbooks of introduction at SAXS (in collaboration with Gérard Fournet) [17] and WAXS [18,15]. These books covered not only technical aspects, but also developed the formalism required to interpret the data. Ref. [15] has been translated in numerous countries and its English version [19] was republished in 1994.

In the following sections, we shall describe the improvement of these pioneering works by successive generations of students from 1940 to 1980. A second (third) section is devoted to SAXS (WAXS) methods to probe short-range order in pure or damaged crystals. A fourth section concerns the determination of local order in ill-organized matter such as amorphous materials and soft matter where both SAXS and WAXS bring complementary information. Finally, section 5 will conclude with Guinier's school nowadays.

---

[1] The term gyration radius proposed by Guinier is not specific to SAXS. This is a typical length first defined in mechanics from the inertial moment I of a rotating object of mass M around an axis passing through its gravity center: $R_g^2 = I/M$. By analogy, in SAXS experiments, the rotation axis is taken along the incoming X-ray beam, the mass density is replaced by the electronic density, and I is the second momentum of the electron distribution function projected in a plane perpendicular to the axis. One thus can use the more precise term "contrast-weighted gyration radius" or "contrast-weighted characteristic length".

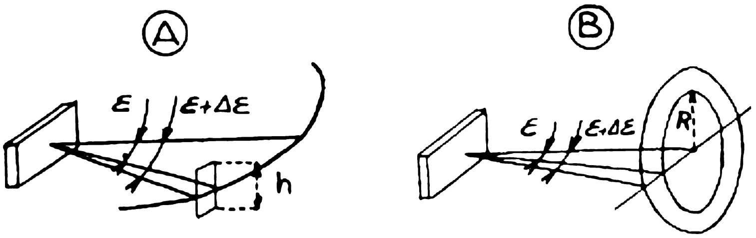

Fig. 3a. Diffracted beam in a conventional horizontal set-up with a vertical divergence h (A) and in the modified set-up allowing the collection of scattering in a crown of radius R and solid angle $2\pi \sin\varepsilon \Delta\varepsilon$ (taken from [23]).

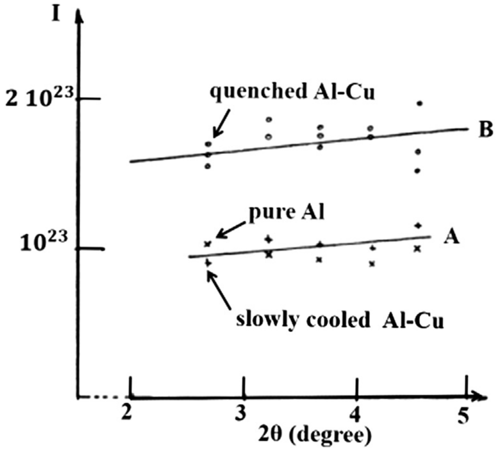

Fig. 3b. Scattering power, I, in Al–Cu alloys as a function of the scattering angle 2θ. A: Thermal and Compton scattering. B: Theoretical scattering power par cm^3 of alloy plus thermal and Compton scattering (adapted from [23]).

2. SAXS studies of localized defects and density fluctuations

The SAXS prototype built by Guinier, shown in Fig. 2b, has been improved to collect information closer to the direct beam. However, this type of set-up has been currently used during many decades, to determine for example in the 1980s the structure of mesophases (see section 4.2) [20].

In the 1960s, SAXS experiments, in continuity with earlier findings, were first devoted to study the first stage of defect formation, namely segregation of Zn atoms in the Al matrix [21] and formation of cavities that are clusters of fluorine vacancies in irradiated LiF crystals [22]. For that purpose, SAXS apparatuses were equipped with a cryostat allowing in situ measurement of samples prepared at 77K: quenched Al–Zn alloys and neutron-irradiated LiF crystals.

However, to reach the required sensitivity to detect scattering by point defects such as foreign atoms, vacancies or interstitials, the conventional SAXS apparatus had to be improved. With defects of size comparable to the one of an atom, the expected low-θ diffuse halo should present a structure factor comparable to the atomic one: isotropic with the azimuthal angle and decreasing slowly with 2θ. Thus, to collect the maximal intensity at constant θ, the scattered beam was detected in a crown of radius R and of solid angle $2\pi \sin\varepsilon \Delta\varepsilon$ (part B in Fig. 3a). This modified detection allows an increase of sensitivity by $2\pi R/h$ with respect to the conventional horizontal detection set-up (part A in Fig. 3a). Then, to keep a monochromatic beam with a point focus, the LiF bent monochromator was pressed on a toroidal surface. The SAXS equipment was completed by a NaI(Tl) detector of large area, which allowed a variation of the 2θ scattering angle between 2.5° and 6°. With this original SAXS apparatus, developed in the 1960s and described in ref. [23], it was possible to measure the intrinsic crystal scattering close to the center of the reciprocal space (superimposed to coherent scattering due to longitudinal phonons and incoherent Compton scattering). Its sensitivity allows one to probe the intensity scattered by density fluctuations in liquids or amorphous materials [24]. This set-up was used to complete previous works concerning earlier stage defects clustering in alloys [23,25] (Fig. 3b), irradiated crystals [23,26], and LiF doped with Ni^{++} [27].

In the 1970s, SAXS studies have moved to the detection of linear trails of damaged materials produced by heavy ions in minerals [28], then to the investigation of lunar feldspar grains hand-picked in several surface soil samples from the Apollo 16 mission. This last study proposed also a new approach for exploiting fossil track records in extraterrestrial materials [29].

The decrease of SAXS activity at the LPS at the end of the 1970s was the consequence of the fact that the original apparatuses used during two decades to study small-size inhomogeneities became outperformed by the building of synchrotron radiation sources and the development of 2D position-sensitive detectors. Note also that, in the 1970s, small-angle neutron scattering (SANS) techniques were rapidly developing and were becoming an unavoidable tool of investigation of organic,

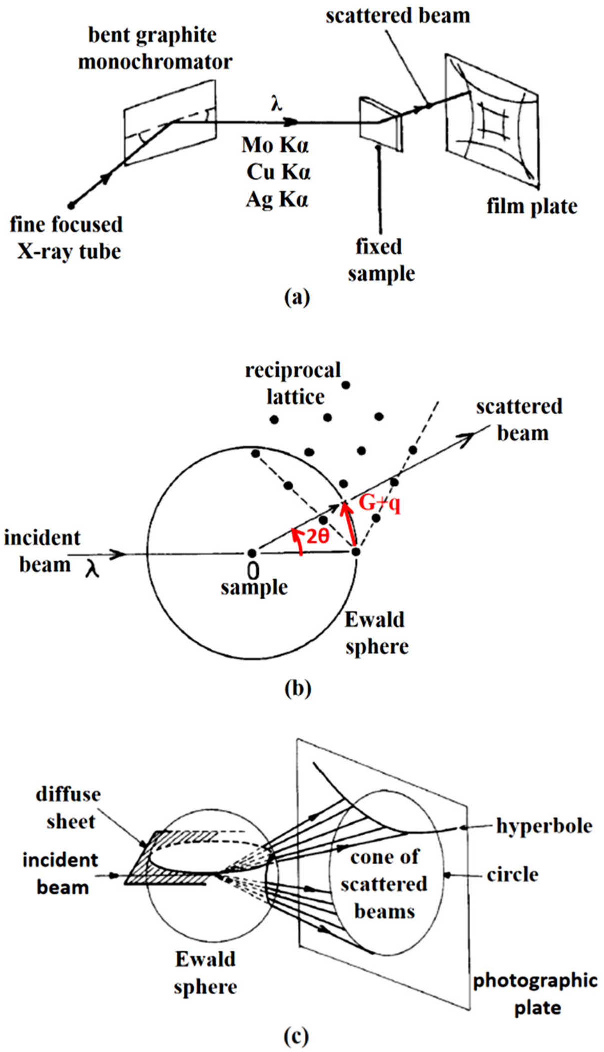

Fig. 4. (a) Scheme of the Laue "monochromatic" set-up developed at the LPS. (b) Representation of a diffraction process in the reciprocal space. (c) Cones of scattered beams due to the intersection of the Ewald sphere with two sets of differently oriented diffuse sheets. The intersection of the corresponding diffraction cones with the planar photographic plate gives rise to different sets of diffuse curved lines.

polymeric and biological compounds by exploiting the contrast between H and D neutron scattering lengths. To finish, let us remark that an important outcome of the development of SAXS apparatus was the use of bent monochromators with point focus, which were also used in WAXS experiments of the LPS until the beginning of the 21st century.

3. WAXS studies of linear short-range order in crystals

Any deviation from the perfect crystalline order gives rise to an X-ray diffuse scattering in the reciprocal space in $\mathbf{G}+\mathbf{q}$ outside of the Bragg reflections located in $\mathbf{G}$. This scattering, generally observed at large 2θ Bragg angle, is detected in WAXS experiments (Fig. 4b). The deviation at the perfect crystalline order is due either to atomic displacement or to atomic substitutions or to a combination of the two effects. The disorder detected by X-ray diffuse scattering method can be either dynamic (lattice vibration) or static (crystalline imperfections). However, conventional laboratory WAXS measurements, where the diffracted beam is recorded without energy resolution, cannot discriminate between these two possibilities. This has the advantage that the diffuse scattering intensity, which is integrated on all the energies, gives directly access to instantaneous spatial correlations of the order parameter η: $S(q,t=0)=|\eta_q|^2$. Here η_q is the q-th component of the Fourier transform of a spatially-dependent atomic displacement wave or density/atomic defect concentration wave.

The X-ray diffuse scattering, of quite weak intensity, was very soon detected on photographic plates used to record Bragg diffraction patterns with a long exposure time (many examples can be found in ref. [15]). At LPS, WAXS experiments were built in the 1960s on the principle of the Guinier chamber where a monochromatic incident beam is obtained after reflection on a bent monochromator allowing a diffracted beam converging on the photographic film (Fig. 4a). Intense incident beams

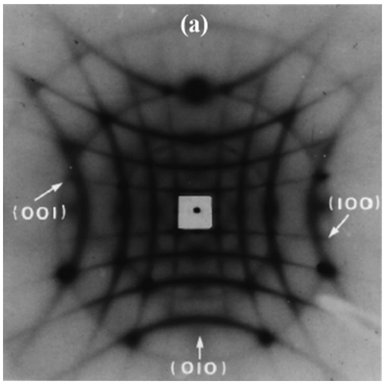

Fig. 5a. The three sets of diffuse line obtained with Mo Kα monochromatic radiation in the para-electric cubic phase of $KNbO_3$ at 500 °C. The [001] axis is parallel to the incident beam, the [100] axis is horizontal and the [010] axis is vertical (from ref. [35a]). The diffuse line spectra contain one set of circles and two sets of hyperboles according to Fig. 4c. It reveals correlated linear Nb atomic displacements along the three uncoupled cubic directions.

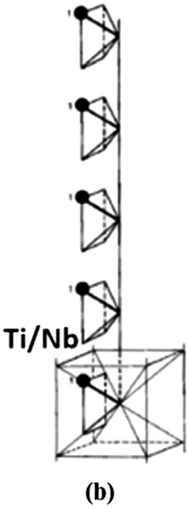

Fig. 5b. In chain correlated uniform shift of the Nb or Ti ion from the center of oxygen octahedron in $KNbO_3$ and $BaTiO_3$. Note that diffraction by a 1D periodic lattice gives rise to planes of Bragg scattering.

were obtained after (002) reflection of the primary beam, produced by a fine focus X-ray tube, on bent pyrolytic graphite monochromators provided by Union Carbide (which were replaced by doubly bent graphite monochromators in the middle of the 1970s). This set-up provides convergent (on the equatorial section of cylindrical photographic films) diffracted beams of high intensity at the expense of a somewhat relaxed angular resolution, which has no real importance to detect broad diffuse scattering in reciprocal space. With a crystal of fixed orientation placed in an incident monochromatic X-ray beam (Fig. 4a), the WAXS set-up provides a survey of large sections of the reciprocal space (the photographic plate reveals cut through several 10 to 100 Brillouin zones; see Fig. 4b) and for this reason this technique was (improperly) named the Laue “monochromatic” method. The difficulty is to obtain X-ray patterns free from contamination due to the parasitic diffraction by elements of the experimental set-up. With a background reduced to the intrinsic diffraction by the sample, integrated on the ellipsoid of resolution of the apparatus, it was possible to detect, at the end of the 1970s, in the low-temperature set up devoted to the study of organic conductors and shown in Fig. 2c, weak diffuse scattering with a signal intensity to background ratio of 10^{-7}. Smaller ratios are now currently obtained with synchrotron radiation achieving a much better resolution and thus a significant reduction in the background.

The high-luminosity Laue “monochromatic” apparatuses developed at the LPS, allowing a large survey of the diffuse scattering in reciprocal space by using a detection via photographic films, were quite unique in the world in the 1970s. Most other laboratories preferred at that time to use the point-counting method allowing a better indexation of the diffuse scattering in $\mathbf{G} + \mathbf{q}$, but with the inconvenient that point detection permits only a limited survey of the reciprocal space. In the 1980s, 1D and 2D position sensitive detectors were developed at the LPS [30] to complete the photographic method by performing more quantitative intensity measurements in WAXS [31] and SAXS [32] studies. Then the conventional photographic plate was progressively replaced by image plate presenting a better linear intensity scale of detection. More recently,

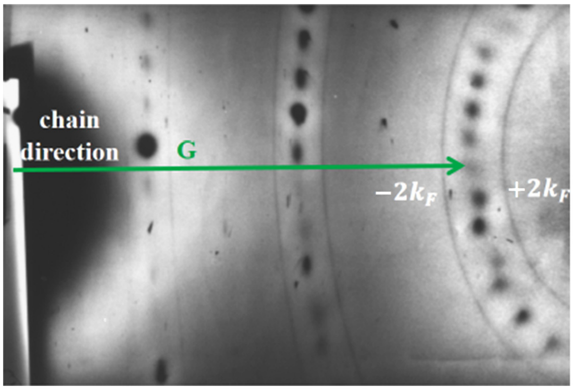

Fig. 6a. WAXS patterns from $K_2Pt(CN)_4Br_{0.3}\cdot xH_2O$ obtained with Mo Kα monochromatic radiation at 300 K. It clearly shows the double set of $\mathbf{q} = \pm 2k_F\mathbf{c}^*$ diffuse lines perpendicular to the chain direction c. The intensity of the diffuse scattering increasing for $\mathbf{c}^*$ (**G** in the figure) increasing is due to a longitudinal modulation of Pt position in chain direction c.

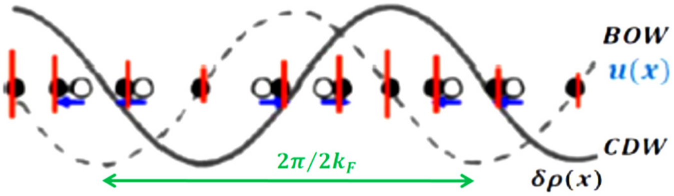

Fig. 6b. $2k_F$ BOW and $2k_F$ CDW modulations in quadrature in the Peierls chain. The diffraction by the 1D $2k_F$ BOW displacement wave of the atomic core $u(x)$ gives rise to two sets of $\pm 2k_F$ diffuse sheets in reciprocal space (adapted from ref. [40]).

2D position sensitive detectors combined with reciprocal space reconstruction algorithms allow a complete and quantitative survey of diffuse scattering.

First WAXS studies were performed in the 1950s in metallic alloys at CNAM then at LPS either in samples previously studied by SAXS (the transformation of quartz into amorphous silica by irradiation with neutron, LiF doped with NiF_2) or in molecular crystals such as naphthalene. However, in these cases, the smooth **q** dependence of the diffuse scattering rendered the analysis of the data quite delicate. The interpretation becomes much simpler when photographic plates revealed in crystals, such as silicon, non-irradiated quartz and perovskites, weak diffuse lines coming from the intersections of the Ewald sphere with diffuse sheets in reciprocal space (Fig. 4c) [33]. This was the unexpected manifestation of linear (chain-like) disorders in the crystal. The most interesting physical situation was the detection of different sets of diffuse lines in ferroelectric perovskites, such as $BaTiO_3$ or $KNbO_3$ (Fig. 5a). Note that the first X-ray diffuse scattering pattern from $BaTiO_3$ revealing these diffuse lines was published in 1965 [34]. These data revealed the existence in the paraelectric phase of these perovskites of three types of interpenetrating chain-like disorder due to three spatially different types of 1D correlated displacements of the Ti or Nb ion from the center of oxygen octahedron (Fig. 5b). These correlated atomic displacements, indicating the presence of local chain-like polarization, are the true precursor of the three successive ferroelectric transitions of these perovskites [35]. These studies, followed by the detection of diffuse sheets or diffuse rods in other families of ABO_3 perovskite (corresponding respectively to the presence of 1D or 2D local atomic correlations [36]), were the beginning of more extensive investigation, revealing the generality of anisotropic atomic correlations as precursors of structural phase transition in cubic srystals. It was shown later, using inelastic neutron scattering [37], that the planar diffuse scattering observed in perovskites is the trace in the reciprocal space of a valley of soft phonons caused by the hybridization of an acoustic branch polarized in the 1D correlation direction with the critical optical mode responsible for ferroelectricity.

The study of perovskites revealed that the LPS WAXS set-up is very well suited for the study of other materials exhibiting chain-like structural instability. This was the case of one-dimensional (1D) inorganic and organic electronic conductors, whose study started all around the world in the early 1970s. In close interaction with experimental studies of electronic properties of the inorganic Krogmann salt $K_2Pt(CN)_4Br_{0.3}\cdot xH_2O$ (KCP), WAXS patterns [38] unexpectedly revealed, in the metallic phase at room temperature (RT), the presence of a double set of parallel diffuse sheets perpendicular to the $Pt(CN)_4$ electronic chain direction (**c**) (Fig. 6a). This set of diffuse lines corresponds to incommensurate 1D correlated fluctuations in chain direction centered around the $\mathbf{q} = \pm 2k_F\mathbf{c}^*$ wave number (k_F is the Fermi wave vector of the 1D electron gas). In KCP, correlated 1D fluctuations involve a longitudinal displacement of $Pt(CN)_4$ entities that modulates the bond distance in chain direction, forming a so-called bond order wave (BOW). Thus, the bond modulation modulates the electronic density, which forms a charge density wave (CDW) in quadrature with the BOW (see Fig. 6b). The WAXS study of KCP evidenced, for the first time, the existence of spatially coherent BOW/CDW in solids. Furthermore, WAXS studies at various temperatures were able to show that, upon cooling to 77 K, diffuse sheets (corresponding to individuals 1D BOW fluctuations at RT) condense into a set of $2k_F$ satellite Bragg reflections, which reflects a 3D interchain coupling between the 1D BOW/CDW RT fluctuations. This structural result, in agreement with electronic measurements, provided the first evidence of the Peierls transition predicted twenty years ago, in the 1950s. In the Peierls mechanism, the interchain coupling stabilizes a 3D lattice of $2k_F$ CDWs with the result of a gap opening at the Fermi level in the 1D band structure. The $2k_F$ 3D structural order is thus also accompanied by a metal-to-insulator transition. To finish, let us remark that the diffuse sheets of $K_2Pt(CN)_4Br_{0.3}\cdot xH_2O$ revealed by Fig. 6a correspond to the trace in reciprocal space of a giant Kohn anomaly formed at the $2k_F$ wave number in the dispersion of longitudinal phonons (for more details, see [39,40]).

Very soon after the discovery of the Peierls transition in KCP, the same type of transition was evidenced around 50 K in the double-stack organic charge transfer salt TTF–TCNQ, where TTF (tetrathiafulvalene) is a donor (D) and TCNQ (tetracyanoquinodimethane) an acceptor (A) of electron [41,42]. However, first WAXS patterns obtained with Mo Kα radiation monochromatized on a LiF crystal exhibited only a weak quasi-1D diffuse scattering above the Peierls transition. The luminosity of the apparatus was thus improved by a factor 25 by using a monochromatic Cu Kα incident beam obtained after (002) reflection on a doubly bent pyrolytic graphite monochromator. Also, the low-temperature set up was rebuilt to achieve a perfect control of the sample temperature and to suppress parasitic contamination (see Fig. 2c). This new set-up allowed one to reveal the unexpected presence of two sets of $2k_F$ and $4k_F$ BOW/CDW diffuse sheets in the metallic state of TTF-TCNQ [43]. The set of $2k_F$ diffuse lines corresponds to a Peierls instability on the TCNQ stack, while the $4k_F$ diffuse lines correspond to a Wigner type of charge localization instability on the TTF stack due to strong electron repulsion (see [40]). The summary, prior to 1980, of Laue monochromatic investigations of 1D conductors is given in refs. [44,45]. After 1980, other kinds of Peierls transitions, also preceded by an important regime of 1D $2k_F$ BOW/CDW thermal fluctuations were discovered by WAXS investigation of different families of inorganic and organic 1D conductors such as the blue bronze ($K_{0.3}MoO_3$) [46], $BaVS_3$ [47] and several families of A_2X or D_2Y organic conductors built with derivatives of TTF or TCNQ, respectively, and where X/Y is a monovalent anion/cation [48]. An interesting situation occurs in 2D conducting Mo and W bronzes where X-ray diffuse scattering investigations show that, contrary to the usual thinking, the electronic structure of the conducting plane is simply the superimposition of three sets of imbricated and differently oriented chains, each exhibiting its own $2k_F$ Peierls instability [49].

As $2k_F$, proportional to the electron 1D band filling, is generally in incommensurate relation with any reciprocal wave vector $\mathbf{G}$, the Peierls ground state of a low-dimensional conductor exhibits an incommensurate modulated structure. In the 1970s, the determination of the pressure–temperature phase diagram of low-dimension conductors and of incommensurably modulated insulators was the object of a considerable attention. At the LPS, studies combining X-ray and neutron diffraction have been focused on organic conductors such as TTF–TCNQ [50] and molecular dielectric insulators such as thiourea [51] and $NaNO_2$ [52], whose ferroelectric ground state is preceded by an incommensurably modulated structure very sensitive to pressure and electric field, and of the di-acetylene PTS [bis-(p-toluene sulfonate) of 2,4-hexadiyne-1,6-diol], primarily studied for its polymerization mechanism [53], whose incommensurate phase is very sensitive to the degree of polymerization.

Two other classes of aperiodic structures, namely incommensurate composite or misfit compounds and quasi-crystals (see section 4.1) were also investigated during several decades by a combination of WAXS and neutron elastic scattering methods. First works on incommensurate composites start around 1976. They concerned non-stoichiometric iodine organic compounds $A(I_3)_x$, where the organic acceptor lattice, A = TTF [54] or TTT (tetrathiotetracene) [45], delimits channels filled by cationic I_3^- species with a repeat periodicity incommensurate with that of the host channel and the inorganic compound $Hg_{3-\delta}AsF_6$ where Hg atoms fill a 2D lattice of interpenetrating channels delimited by the AsF_6 [55]. An original aspect of several $A(I_3)_x$ systems [56,57,31] is that incommensurate iodine column, not coupled with its neighbors, behaves as a 1D liquid at RT. In that case, diffraction gives rise to a set of periodic diffuse lines on the photographic plate (Fig. 7) corresponding to the intersection of the Ewald sphere with diffuse sheets due to the diffraction by uncoupled I_3^- columns (Fig. 4c). Misfit order of the chain of dopant with respect to the polymeric chain was also observed in highly conducting forms of polymer such as iodine-doped polyacetylene [58]. Recently, misfit arrays of chains of fullerene embedded in a single-wall carbon nanotube [59] were also reported. Misfit order is also observed in intercalated graphite and in some of them the intercalate layer behaves as a 2D liquid at RT [60]. Misfit orders are also commonly found in soft matter (see section 4.2).

Examples of WAXS studies posterior to 1980 are covered by several reviews [61–66]. Today X-ray diffuse scattering studies are greatly facilitated using synchrotron radiation, which provides an incident beam of higher intensity and better resolution than conventional X-ray tubes. Also, modern data acquisition techniques allow us to reconstruct oriented portions of the reciprocal space (which is not the case with the recording on steady photographic films used in the earlier “monochromatic Laue” method). Numerical methods also allow us to simulate experimental WAXS pattern from microscopic models of disorder. For example, this method has been used with success at the end of the 1990s to determine inter-fullerene interactions [67]. Also, WAXS measurements coupled with numerical simulations allow us to determine, for example, the organization of an assembly of individual nano-objects such as carbon and inorganic nanotubes or their confinement in host systems such as zeolite channels [66].

To finish, let us mention that interferences due to the coupling of a displacement modulation wave with a composition modulation wave in a solid solution modify in an original manner the WAXS spectra. It produces diffuse scattering of asymmetric profile or even forms in the extreme case of 1D systems a set of “white diffuse lines” where the intensity is

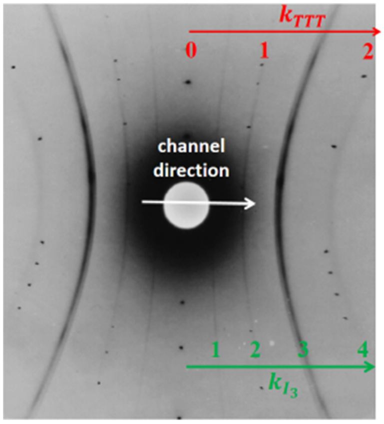

Fig. 7. Very first WAXS pattern obtained in 1978 with the synchrotron radiation of LURE (Orsay) from the misfit organic salt $(TTT)_2I_{3+\delta}$ at RT [56]. Continuous lines are due to diffraction by non-correlated iodine chains, while sharp spots correspond to the Bragg diffraction by the 3D organic host lattice. Because of the non-stoichiometry of the compound ($\delta \neq 0$) diffuse lines (indexed by $k_{I_3} \geq 1$) are located outside layers of Bragg reflections perpendicular to the channel direction (indexed by k_{TTT}). With the good resolution of the synchrotron radiation, the misfit of lattice parameters between iodine and organic acceptor sub-lattices in channel direction ($b_{I_3}/b_{TTT} \approx 1.97$) is clearly visible at large Bragg angles. The Miller index $k_{I_3} = 3$ of the strongest intensity diffraction line reveals the presence of I_3 species.

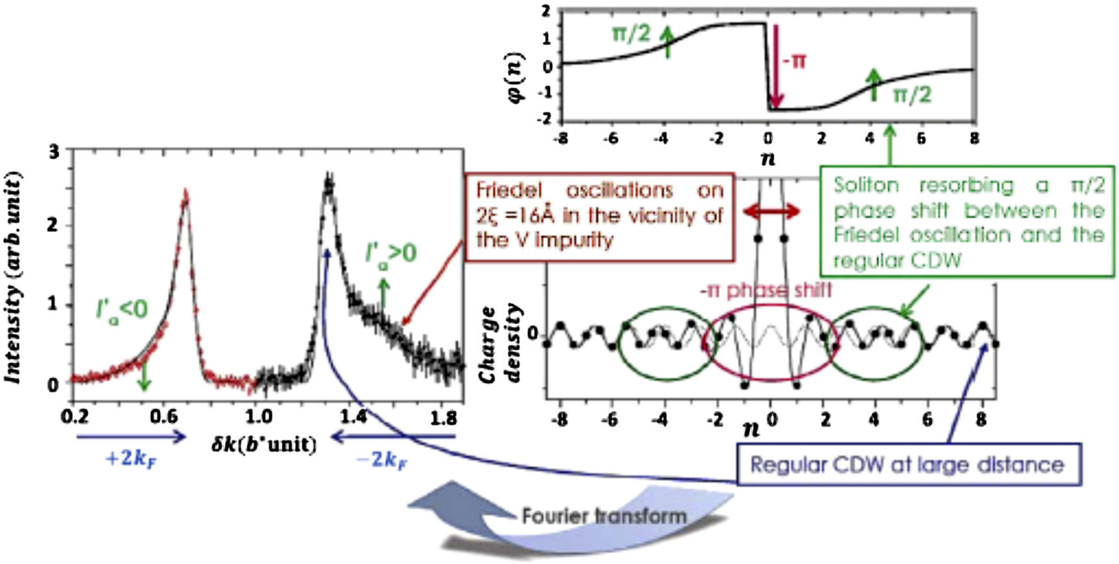

Fig. 8. Longitudinal section of the $\pm 2k_F$ asymmetric diffuse lines from $K_{0.3}(Mo_{0.972}V_{0.028})O_3$ (left side of the figure) compared to the Fourier transform (continuous line) of the pinned BOW/CDW in a V impurity (placed in $n = 0$) and represented on the right-hand side of the figure. (Adapted from ref. [71]; for a complete explanation of the figure, see ref. [40].)

subtracted from the part of the background due to Laue scattering from disorder in the solid solution [68]. The sign of such interferences allows one to determine the phase shift between the two coupled modulations. The basic aspect of this interference effect can be simply explained [68] using the formalism developed by Guinier in the 1950s [15,69]. This effect, due to the diffraction by two modulation waves in quadrature, also bears some analogy with holography in optics [70]. Since its first report in 1992, this effect appears to be quite general in disordered materials. Profile asymmetry can also be noticed in earlier SAXS spectra evidencing the formation of GP zones [70]. “White diffuse lines” and the presence of GP zones are also observed in soft matter (see section 4.2). Also, this interference effect has been used to characterize the pinning mechanism of BOW/CDW on defects or substituent. Fig. 8 illustrates such a mechanism via the formation of Friedel oscillations, accompanied by a π phase shift (screening of the excess of charge of the non-isoelectronic V impurity) in the substituted blue-bronze $K_{0.3}(Mo_{1-x}V_x)O_3$ [71].

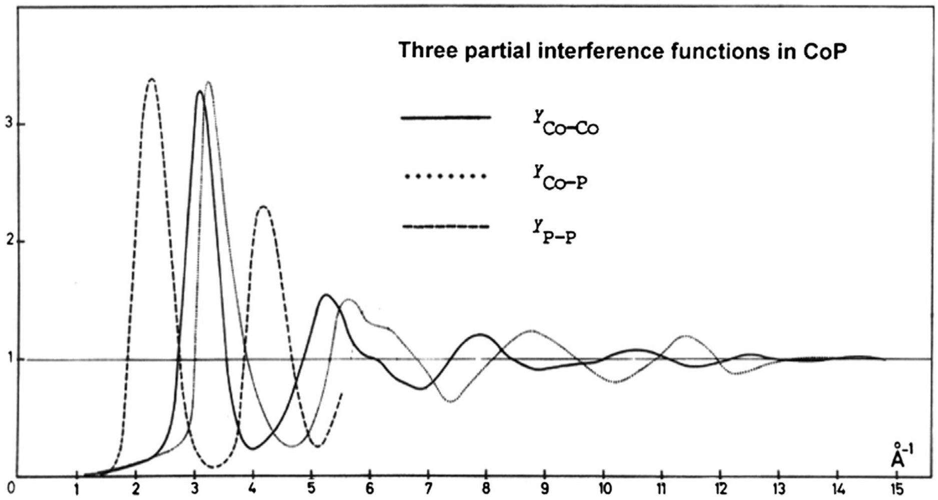

Fig. 9. Partial interference functions in the metallic glass $Co_{81}P_{19}$ using a combination of conventional X-ray laboratory and neutron diffraction data. In the neutron diffraction process, both nuclear and magnetic scattering are contributing to the analysis.

4. Locally organized matter

4.1. Amorphous materials

Research on amorphous metals started at the LPS when, after coming back from a stay at Caltech, Jean Dixmier introduced in the late 1960s the technique of ultra-fast quenching of metals consisting of cooling a liquid metal alloy at about 10^6 degrees per second. During his stay, he visited Pol Duwez, who obtained the first amorphous alloy ($Au_{80}Si_{20}$) in 1957, and who was also the first to understand that alloys with a deep eutectic composition in the phase diagram are good candidates for amorphous metallic alloys [72]. Guinier was rapidly convinced that this technique [73] should open a new door toward several domains of metallurgy: solid solutions in metallic alloys, amorphous metals and, some years after, the revolution of quasicrystals. Materials produced at the LPS were studied by structural techniques (X-rays, neutron diffraction, electronic microscopy…), but also for their magnetic, thermodynamic, and electronic properties. These researches were done in collaboration with several teams all around the world (USA, Great Britain, Japan, Italy, Yugoslavia, etc.).

At the beginning, a rapid quenching method from the melt produced small samples whose size was increased later by quenching on a rotating cooper wheel able to achieve long ribbons. However, to produce larger sample required for neutron diffraction studies, electrolytic deposition appears to be a good method of preparation of amorphous alloys such as CoP, NiP. These materials were very well suited to perform neutron diffraction studies in the new facility built at Grenoble in the 1970s in the framework of a collaboration between France and Germany: the “Institut Laue Langevin” (ILL).

Fig. 9 gives an example of experimental determination of partial interference functions in the metallic glass CoP which combines X-ray and neutron diffraction methods [74]. From these partial functions it is possible to extract the contribution of different kinds of atomic pairs to the scattering process and thus to describe the local order in a binary glassy metal, as illustrated in Fig. 10 for CoP. Understanding from structural experiments the coupling that drives metallic systems toward their local structure has been achieved at the LPS by structural simulations [75,76] and by electronic structure calculations (André Blandin and Jacques Friedel).

From these results it appears clearly that the local order was icosahedral around metallic atoms (Fig. 10). Then modeling structures with this type of local order was introduced simultaneously in Guinier’s team [75] and in several laboratories, especially in Great Britain [77]. However, it is well known in classical (periodic) crystallography that icosahedral symmetry is impossible. So, the crucial question was how to propagate such a local order by introducing disorder in respecting observed macroscopic properties such as the density? The simplest approach, following paracrystal models developed at the end of the 1940s, was to consider amorphous structures as conventional crystalline structures where “disorder” broadens Bragg diffraction. This idea displeased Guinier, who was convinced that the effect of defects is subtler than simply blurring a periodic array. Structural defects, as vacancies, dislocations…, are in the scientific culture of the LPS, where their influence on the crystal structure has two complementary aspects: a metric-induced lattice distortion but also a topological (in the mathematical sense) characteristic. To define a topological defect, one needs to have a perfect reference state. For instance, dislocations are defined relatively to perfect crystals and topologically characterized by their Burger vectors. The icosahedral local order, as the one found in binary glassy metals (Fig. 10), which is incompatible with crystalline order, rules out any reference to a crystal. In the present case, one needs to define a perfect icosahedral reference structure. This debate with Guinier allowed one of us (JFS) to propose the use of structures in non-Euclidean spaces where icosahedral order is possible [78]. A simple example, illustrated in Fig. 11, helps to follow the reasoning. Suppose that you want to perform a planar tiling by regular pentagons. Again, two-dimensional classical crystallography tells you that this is impossible (left-hand part

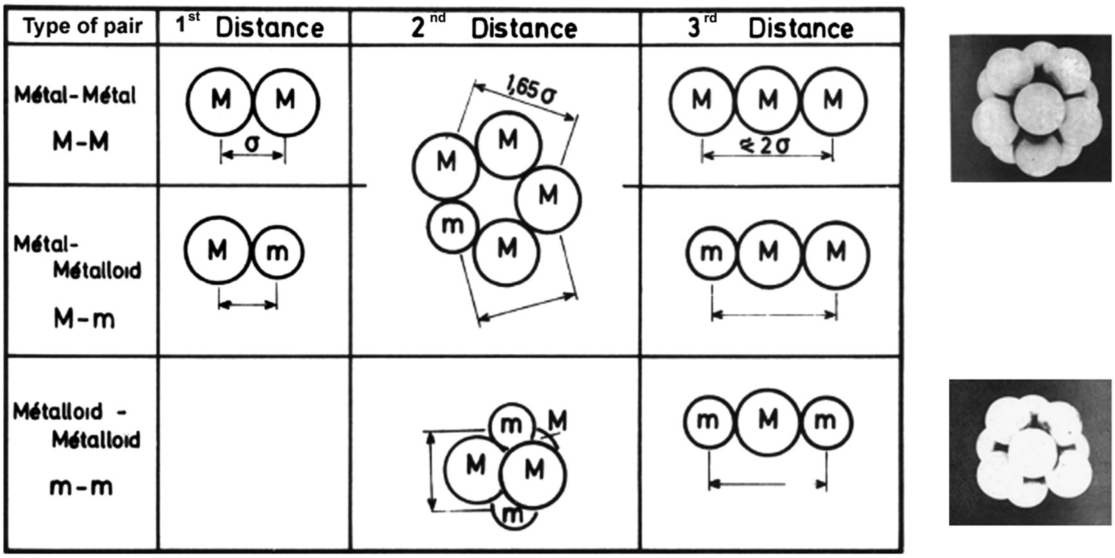

Fig. 10. Types of local order in a binary glassy metal like CoP (left side). The right-hand side shows some models of icosahedral coordination around metallic atoms and coordination around metalloid atoms (9 neighbors). Such structures have been modeled by packing of hard spheres with two diameters respecting the local coordination rules.

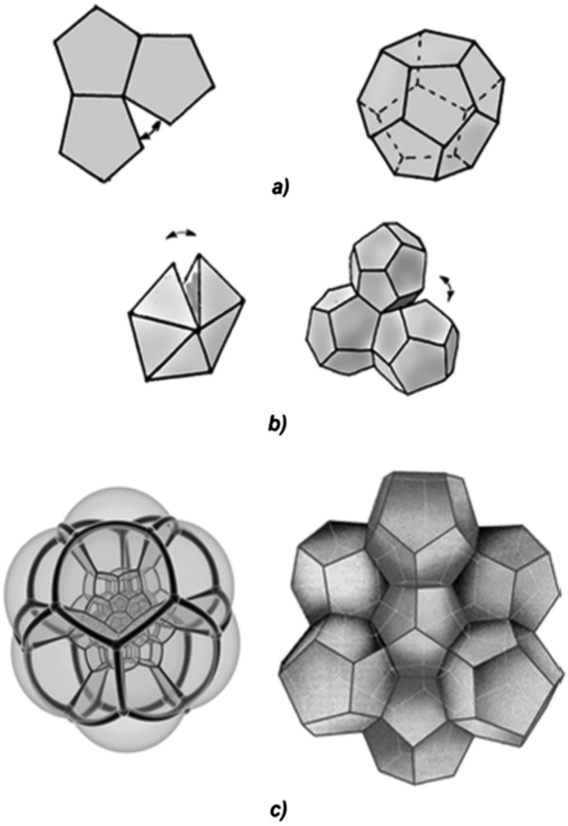

Fig. 11. a) It is impossible to tile planes with regular pentagons (left side), but it possible to tile the sphere with pentagons by forming a dodecagon (right-hand side). b) In a similar way, it is impossible to tile Euclidean space with tetrahedra or dodecagons (the Voronoi cell for atoms with icosahedral coordination shell), but there are tiling solutions in locally curved space, as schematized in (c).

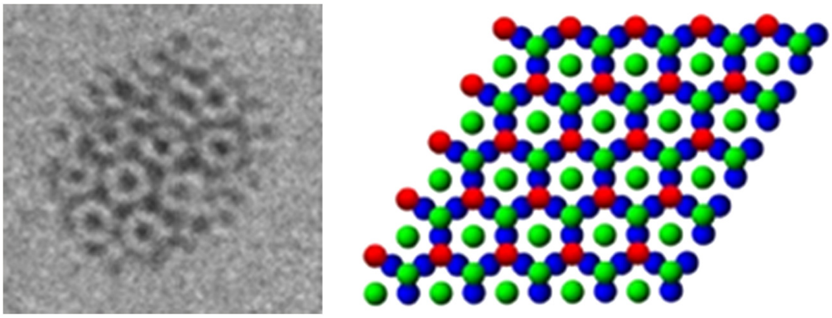

Fig. 12. Left part: small grains of hydrophobically coated gold nanoparticles in a superlattice grown in an oil–water emulsion and forming the C14 Frank–Kasper phase shown in the right-hand part of the figure (from ref. [82]).

of Fig. 11a). However, you have this possibility for a 2D curved surface, because pentagons can tile the sphere by forming a regular dodecagon (right-hand part of Fig. 11a). Thus, tiling of the plane with pentagons should necessarily introduce defects relatively to this curved regular structure. Similarly, Fig. 11b shows that it is impossible to tile Euclidean space with regular polyhedra such as tetrahedra or dodecagons, but there are tiling solutions in locally curved space, as schematized in Fig. 11c. Thus, with a perfect reference structure in curved space, it is possible to analyze a real structure in Euclidian space in terms of defects. In the examples considered previously, defects are disclinations (a defect in rotational symmetry) whose structure is perfectly well understood. During the 1980s, these types of defects were well known in soft matter, but not in metallurgy.

Finally, the discovery of quasicrystals reported in 1984 [79], but first observed by electron microscopy in 1982, was a flash of new ideas to which André Guinier has participated with enthusiasm (this was not always the case for all the great leaders in crystallography of his generation). In collaboration with other teams in France, the LPS started to be a very active center in that domain [80], not only with the structural point of view, but also with consideration of the quantum aspects of the stabilization of quasicrystals [81].

The school of thought that André Guinier has been able to orient and to accompany with flexibility, has scientific extension until now. We give below a clear example of the fruitful aspect of imbrications in diversified fields of research at the LPS: quasicrystals and related complex structures like Frank–Kasper phases can be relevant to understand the “soft matter” array, a surprise for the metallurgist! Although the Frank–Kasper phases were already known before the discovery of quasicrystals, their complex architecture is now considered as making a link between simple close-packed periodic structures and some quasi-periodic structures. These tetrahedral close-packed structures are observed in many materials from simple elements to intermetallic compounds, but also in self-assembled soft-matter materials like micellar systems, dendritic liquid crystals, star polymers, and, more recently, block copolymers or gold nanocrystal superlattices. An example is shown in Fig. 12.

4.2. Soft matter

After 1968–1969, several members of the LPS joined Pierre-Gilles de Gennes’ new activity concerning the physics of liquid crystals (or, as named by Georges Friedel, mesophases). The development of this new field of research required a tight collaboration with chemists, which on their own explored the vast domain of mesogenic substances. With these researches, the number of intermediate phases separating the anisotropic liquid (or nematic) from classical crystalline phases increased considerably. Structural experiments then became essential to understand the molecular organization in these phases. These studies have followed two different paths.

- When mesophases are formed in binary mixtures of surfactant molecules and of water (lyotropic phases), the structure is described by that of the surface separating two non-miscible media. The structure of the mesophase depends upon the geometry of this surface and varies with the composition of the mixture.
- A certain number of pure compounds, when heating the perfect crystalline phase, show a few numbers of distinct phases, called mesophases. These mesophases are more disordered than a perfect crystal, but less than an isotropic liquid. These compounds, called thermotropic mesogens, are organic molecules of high molar mass (between one hundred and more than one thousand proton masses). Structural studies, using the same technique of investigation as for crystal, aim at determining how individual characteristics of molecules influence the symmetry and local organization of the mesophase.

In the earlier time, the determination of mesophase structures was done by analysis of powder patterns [83]. Typical X-ray patterns exhibit few (1 to 10) sharp rings, all located at small Bragg angle, and a broad peak at larger angle. The set of sharp rings indicates the presence of a periodic array whose dimension depends on the molecular organization in the mesophase: 1D for lamellar or smectic phases, 2D for assemblies of cylinders, and 3D for interfaces of various shapes.

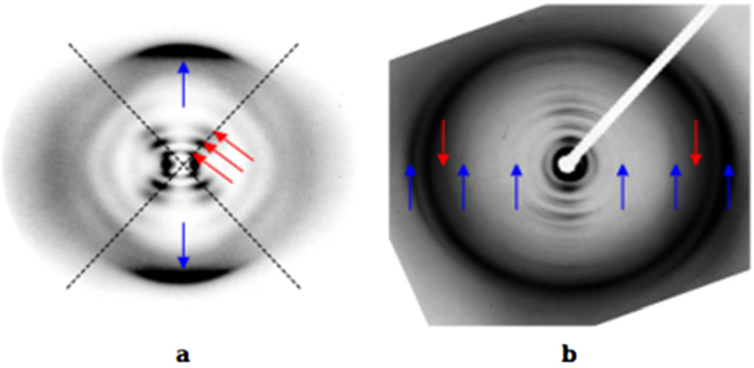

Fig. 13. Diffraction patterns showing the presence of a large period modulation along the column direction. (a) Fiber of a mixture DNA/water in a hexagonal mesophase. The blue arrows show diffraction arcs due to the stacking of bases. The red arrows are supplementary reflection characteristics of the double helix structure (from [90]). (b) Central part of the diffraction pattern of a hexagonal phase of fibers. Blue arrows show meridian arcs corresponding to the regular stacking of molecules in a column. The supplementary red arrows indicate the existence of a density modulation in the column direction (from [92]).

Whatever the dimension, this period is controlled by the largest dimension of the molecular components (i.e. of the order of a few nanometers). Nevertheless, the number of visible sharp peaks is limited by a large attenuation factor due to both static and dynamic structural disorder and the major part of the diffracted intensity comes from different diffuse zones that can be evidenced on patterns of aligned samples (single domains or fiber-like texture). The broad feature, corresponding to a typical interatomic distance $d \leq 0.5$ nm, characterizes the "liquid" aspect of the molecular organization.

Nearly all mesogens studied during the 1970s had a rod-like shape and form nematic and smectic phases. However, some of them exhibited a complex polymorphism. There the first step of transformation between the "perfect crystal" and fluid mesophases, classified as smectic (lamellar) phases, belongs to the class of orientation disordered crystals. For example, the terephthal-bis-butylaniline molecule (TBBA) exhibits a phase transformation at 113.5 °C, which is easy to detect with single-crystal diffraction methods. The molecules are organized on a monoclinic $C2/m$ network, the c parameter is of the order of the molecular length, and each layer is made of parallel rod-like molecules closely packed on a slightly distorted 2D hexagonal lattice. However, the diffraction pattern shows a limited number of visible Bragg reflections together with a strong diffuse scattering outside of reciprocal nodes. The diffuse intensity is mainly localized in diffuse sheets perpendicular to the molecular long axis [84] and passing through diffuse spots located in the $(hk0)$ plane at special positions of the Brillouin zone boundary. Upon cooling, the sample transforms into a metastable phase at ~90 °C with a change of symmetry ($P2_1/a$) driven by a variation of the mean molecular shape and the "in-layer" structure becomes a herringbone array of platelets. Moreover, the diffuse spots of the high-temperature phase are the signature of a local herring bone array. A complete study of this cycle of phase transformation using both X-ray and coherent neutron diffuse scattering on both hydrogenated and deuterated single crystals is reported in [20]. This clarifies the progressive evolution of disorder in mesophase of rod-like mesogens [85,86]. Reanalyzing in 1990 the previous X-ray diffraction patterns with a new perspective, opened by the analysis of the solid solution of organic conductors [68] (see the end of section 3), it appears that a central "white line" is systematically inserted in the set of gray diffuse lines previously mentioned. By combining all these features, the periodic diffuse sheet array thus appears to be the reciprocal image of a linear Guinier–Preston zone in which a molecular vacancy is surrounded by a linear delocalized interstitial [87]. Such linear defects originate from the coupling between the intra-layer disorder (herring bone array) and off layers interactions. Similar coupling exists in fluid smectics [88].

In the true liquid-crystalline phases, the analysis of the X-ray pattern differs from the dimensionality of the periodic lattice.

For a 2D assembly of cylinders, all the Bragg reflections are localized in the equatorial plane and the diffuse scattering pattern is the reciprocal image of the cylinder. The most famous image obtained in this case is the diffraction pattern of DNA in the gel state. In the gel, there is no interaction between neighboring parallel molecules: the diffraction pattern is that of a single molecule (it shows the double helix form factor [89]). More than thirty years after, Françoise Livolant, studying the liquid crystalline properties of lyotropic suspensions of DNA by optical and electronic microscopes, was able to identify two different liquid-crystalline states in mixtures of molecules of calibrated length in water. The most ordered phase was identified by X-ray diffraction experiments on aligned samples as a columnar hexagonal mesophase and, due to this fact, the form factor of the DNA polymer (in its B form in gels) simply appears on the diffraction pattern (Fig. 13a) [90]. A similar diffuse pattern appears superimposed over the diffraction spots of single crystals of a DNA oligomer: some DNA molecules in B conformation are inserted in the crystalline matrix of A form DNA molecules [91]. Other examples of an incommensurable modulation of the distribution of molecules along the column axis have been evidenced. The signature of a helical array is visible in the diffraction pattern of a single domain of a disc-like compound [92]. In a third example of hexagonal columnar mesophase, an incommensurate density modulation is observed along the column axis [93] (Fig. 13b). In this case, the structure of a column is related to the complex dendrimeric architecture of the molecule.

A last example illustrates the impact of the presence of localized defects in the column array architecture on the nature of the mesophase. The studied compounds belong to a series of molecules forming anisotropic structures by assemblage. The central part is a single benzene ring on which are attached two amide groups (–NH–CO–). Amide groups of two molecules are linked by H-bonds (Fig. 14b). Different groups, such as long paraffinic chains, complete the molecule, giving it a mesomorph character. Rigid wires (or columns) surrounded by melted chains are thus obtained [94]. One molecule is particularly interesting, because it passes through two mesomorphic states. At low temperatures, the rigid columns of circular sections are parallel and are located on the sites of a hexagonal planar lattice. At high temperatures, the phase is nematic: columns remain approximately parallel, but there is no long-range order in the plane perpendicular to the columns. From the distribution of diffracted intensity by aligned samples, it is possible to obtain the distance between molecules in the column direction and the distance between two columns in the perpendicular plane. A comparison with lattice parameters deduced from diffraction experiments and with the molecular volume measured by dilatometry gives the average number of molecules per unit cell. It is less than unity in the low-temperature hexagonal phase and 1.15 in the nematic phase. If this system is assimilated to a crystal, these findings imply the presence of localized defects. Thus, the hexagonal phase contains vacancies that progressively transform into interstitials [95]. SAXS measurements allow one to assess this interpretation [32]. Inside the first Brillouin zone, the scattered intensity is isotropic and independent of the modulus of the scattered vector. There is also a correlation between the evolution of the volume fraction of defects and the SAXS cross section (Fig. 14a). The most striking effect is the decrease of the scattered power when the isotropic liquid phase is reached. It is thus reasonable to assume that, in the two mesophases, a first contribution comes from the disordered medium of paraffinic chains, while a second one comes from less mobile defects. The construction of columns via H-bonds is responsible for the "solid" properties of the mesophase. Defects, vacancies and interstitial can be described as topological defects (a π defect is shown in Fig. 14b), which, in this peculiar example, play a fundamental role in the transformation of the hexagonal phase into a nematic one. However, the magnitude of the density fluctuations of the so-called "liquid component" is lower than the one observed in a medium of melted free alkanes. An analysis of the "liquid state" should consider more realistically the conformational disorder of the alkyl chains probed by NMR experiments [96].

The diffraction patterns of fluid lamellar phases (1D periodic order) are indicative of local displacement of small clusters of molecules out of the mean position. An especially complex X-ray pattern is obtained with smectic A phases of comb-like liquid-crystalline polymer where mesogenic groups are linked to a polymeric backbone through flexible spacers. In this smectic A mesophase, mesogenic side-groups form liquid-like layers, with a mean orientation perpendicular to the layer planes, and each layer is made of three sub-layers: the polymeric backbone, the spacers, and the terminal mesogenic groups [97]. The aligned smectic phase of polymetacrylate, PMA (Fig. 15c), presents quite a complex diffraction pattern (Figs. 15a and 15b, and schematically represented in Fig. 15d). Bragg reflections (a) and large angle arcs (b) are observed, forming the two main features of a smectic A phase. The set of diffuse lines (c), the four broad spots (d), and the diffuse streaks (e) correspond, respectively, to a displacement of the column of monomers, to local undulations of layers and to a local bilayer structure [98]. In Fig. 15b, which corresponds to an overexposed pattern, a sharp line of weak intensity (f) with an unusual curve of "mustache-like" shape appears [98]. It originates from the backbone that crosses the layers with an average of one-layer crossing per macromolecule. Crossings are surrounded either by a nematic zone or by a local distortion of smectic layers. The characteristic of the diffuse line (f) is consistent with the geometric model of local distortion of smectic layers, as shown in Fig. 15e. The apparent width of the defect is 2 nm, and its length is of the order of ten times the layer thickness; consequently, these defects are the superposition of several individual "layer-crossing" macromolecules.

General reviews on topics outlined above are found in references [88,99,100]. Another interesting set of study performed in collaboration between the LPS and the LURE synchrotron radiation source concerns X-ray diffuse scattering investigations of crystals of biological molecules [101].

Finally, it is interesting to note that the study of organic mesophases has been extended during the 1990s to mineral systems, such as clays, with colloidal suspensions of anisotropic (nanotube, disc, ribbon, platelet...) nanoobjects [102]. Hybrid mesophases such as liquid-crystal phases doped with mineral nanoparticles have been also studied. Very original phases are observed in hydrophobically coated gold nanoparticles (see Fig. 12).

5. Conclusion: Guinier' school nowadays

The transfer of Guinier's team in 1959 on the campus of Orsay in the future "Université Paris-Sud" (now "Université Paris-Saclay"), first in Building 210, then in 1970 in Building 510 on the "Plateau de Saclay", was the occasion to develop research by an easier recruiting of students. Fig. 16 is a photograph of Guinier with the X-ray group in 1978.

In spite of the increase in size of the "X-ray" team, the way to perform research remains largely inspired by Guinier's pioneering works based on the development of an original instrumentation (often unique in the world at that time) adapted to obtain clear-cut experimental results completed by the use of a pertinent formalism to provide a clear physical interpretation of the data. Researches were also performed in a pragmatic manner to obtain a precise understanding of the (local) organization of matter taking into account the role of defects and instabilities, even if it contradicts what the majority of the community was believing. This approach is opposite to the one consisting of performing experiments to verify an established theory. Guinier was very fond of the advice of William Lawrence Bragg "Never hesitate to do an experiment that the theoreticians have declared stupid".

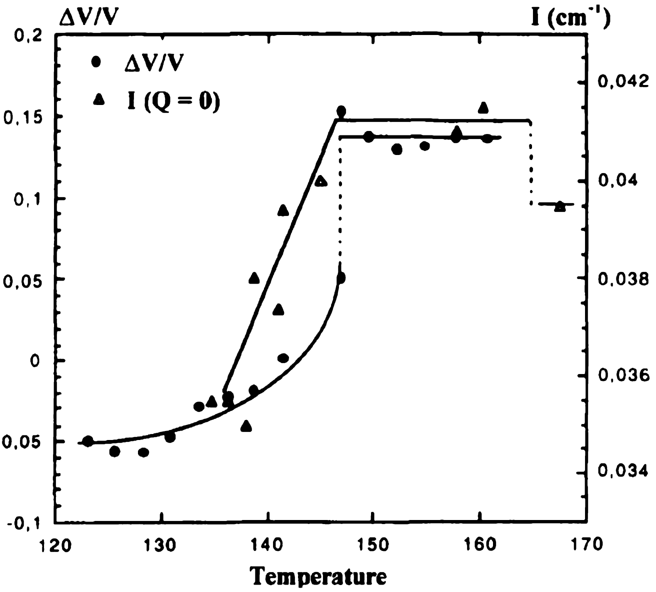

Fig. 14a. Temperature dependence of $\Delta V/V$, the volume fraction of defects, and of I, the SAXS cross section.

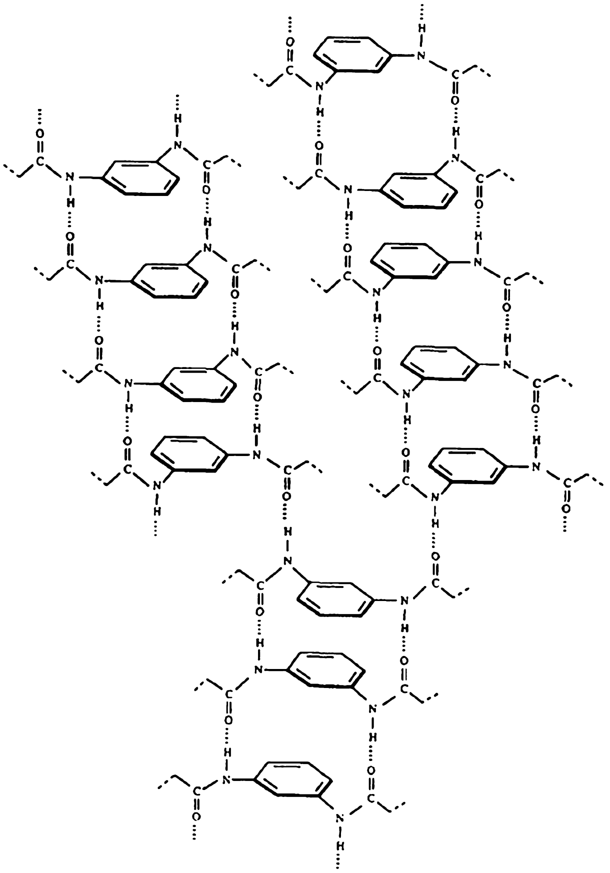

Fig. 14b. Schematic representation of the hydrogen bonds array around a π defect.

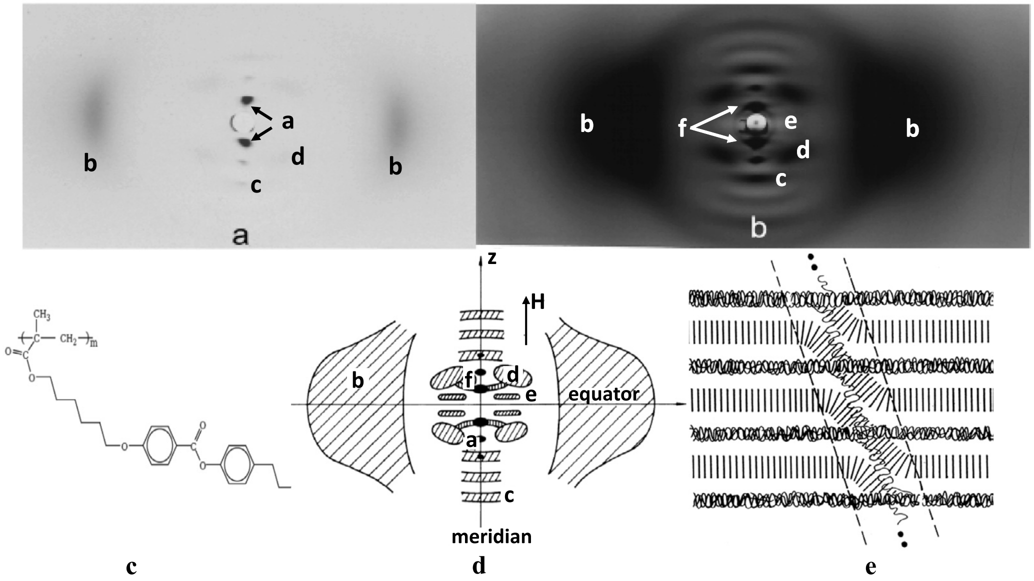

Fig. 15. Low-exposure (a) and high-exposure (b) diffraction patterns from aligned PMA whose molecule is shown in (c). (d) Schematic representation of the total diffraction pattern. Letters “a” to “f” refer to the different types of reflections discussed in the text. (e) Local deformation of the smectic layer array at the origin of scattering “f”.

André Guinier was very rigorous with his students on the condition of obtention of the data and of their analysis. Every detail should be considered, analyzed, and explained in a critical manner. This renders the life particularly difficult when unexpected X-ray diffraction patterns were obtained. However, it is by insisting on having an interpretation of all the results that do not fit with what is expected, that novel directions of research are often open. Remembering his scientific life, André Guinier wrote in 1999 an interesting tribune entitled “As chance would have it…” [103]. Chance is important in research, but only a prepared mind has a better opportunity to make use of it. The role of a school of thought, as the one created by Guinier, is to prepare the minds

Nowadays conditions of performance of SAXS and WAXS experiments have drastically changed with the generalized use of synchrotron radiation facilities and the development of X-ray free electron laser (XFEL). With a panel of available new techniques, laboratory work is now used to prepare elaborated experimental investigations on large-scale facilities. To name a few, diffraction techniques developed for the synchrotron radiation, allow, among some recent topics investigated by the X-ray group of the LPS:

- using the high-resolution and high-luminosity characteristics of the synchrotron radiation, to record the powder spectrum (free from twinning effect) of modulated structures [104] and of collection of nano-objects [105],
- recording high-resolution SAXS patterns for studying very long period structures [106],
- using the extremely narrow beam size to record WAXS patterns under high pressure [107],
- using inelastic X-ray scattering to analyze the energy dependence of the X-ray diffuse scattering,
- using the fine-tuning of the wavelength of the incoming beam to perform resonant (anomalous) X-ray diffraction [108, 109]*,[2]
- using the magnetic X-ray scattering to determine magnetic structures [110],
- using the coherence of the synchrotron radiation to reveal localized defects in LRO structures [111],
- using the pulsed nature of the synchrotron radiation to perform time-dependent diffraction [112].

Finally, one should not forget the complementarity between the X-ray and neutron scattering techniques, which has been fruitful in the past to study dynamics of phenomena associated with X-ray diffuse scattering features (many examples are given in this paper). This complementarity remains useful today to study strongly correlated systems where there is a subtle interplay between charge, spin, orbital and lattice degrees of freedom probed differently by X-ray and neutron scattering

---

[2] In liquid crystals, periodic orientation order uncoupled with any position modulation is observed. If the modulation period is in the range of the wavelength of visible light, the structure can be analyzed by the diffraction technique owing to the variation of the dielectric susceptibility with local molecular orientation (cholesteric and blue phases). For shorter periods (∼10 nm), diffraction peaks are revealed using the tensor property of the atomic scattering factor. In this case, resonant diffraction offers a new method of investigation of chiral liquid crystalline phases, which could be generalized to any mesogene using the resonance at carbon K-edge.

Fig. 16. A. Guinier and the X-ray group below the oak of the building 510 in May 1978. (First raw: J. Doucet, J.-M. Dartyge, F. Denoyer, D. Taupin, A.-M. Levelut, C. Taupin, A. Guinier, M. Lambert, M. Cagnon, C. Defrance J. Dixmier; Back raw: J. Ferré, J.-C. Malaurent, S. Megtert, L. Gatebois, A.-M. Quittet, J.-P. Pouget, A. H. Moudden, R. Comès, G. Sauvage, P. Meyer, P. Lagarde, A. Guillory).

techniques. This is, for example, the case of multiferroicity, which combines ferroelectric and ferromagnetic orders involving hybrid excitation having both phonon and magnon character.

To conclude, let us point out the international audience of André Guinier these days for its pioneering work in the development of SAXS and WAXS techniques, which are crucial tools of investigation of local orders in condensed matter. His reputation also comes from his will to disseminate basic concepts of these techniques through textbooks [15,17–19], continuously enriched by original experimental studies performed by himself and his team. Another important aspect of Guinier's achievement relies on his interest in vulgarization. In this respect, he published in his late days several books on X-rays and the structure of the matter, written first in French and then translated into English for the two last ones [113–115], where he achieved the "tour de force" of transmitting recent scientific results to a large audience in an elegant and simple manner.

Acknowledgements

Authors are grateful to P. Davidson, P. Foury-Leylekian, P. Launois, N. Mehl, D. Petermann, and S. Ravy for providing useful information during the writing of this paper.

References

[1] S. Ravy, A. Guinier, (1911–2000): a physicist among crystallographers, Phys. Scr. 90 (2015) 038001.
[2] A. Guinier, La diffraction des rayons X aux très petits angles : application à l'étude de phénomènes ultramicroscopiques, Ann. Phys. 12 (1939) 161.
[3] A. Guinier, Personal reminiscences, in: P. Ewald (Ed.), 50 Years of X-Ray Diffraction, International Union of Crystallography, Springer, 1962, pp. 574–578.
[4] A. Guinier, Dispositif permettant d'obtenir des diagrammes très intenses de diffraction des poudres cristallines avec un rayonnement monochromatique, C. r. hebd. séances Acad. sci. 204 (1937) 1115.
[5] A. Guinier, La diffusion des rayons X sous les très faibles angles appliquée à l'étude de fines particules et de suspensions colloïdales, C. r. hebd. séances Acad. sci. 206 (1938) 1374.
[6] A. Guinier, Un nouveau type de diagrammes de rayons X, C. r. hebd. séances Acad. sci. 206 (1938) 1641.
[7] A. Guinier, Structure of age-hardened aluminium–copper alloys, Nature 142 (1938) 569;
G.D. Preston, Structure of age-hardened aluminium–copper alloys, Nature 142 (1938) 570.

[8] G.D. Preston, The diffraction of X-rays by age-hardening aluminium–copper alloys, Proc. R. Soc. 167A (1938) 526;
G.D. Preston, The diffraction of X-rays by age-hardening aluminium–copper alloys. The structure of an intermediate phase, Philos. Mag. 26 (1938) 855.
[9] M. Winterberger, Les zones de Guinier-Preston ont 50 ans, Cahiers d'histoire de l'aluminium 3 (1988) 37, avec réponse d'A. Guinier.
[10] A. Guinier, On the birth of GP zones, Mater. Sci. Forum 217 (222) (1996) 3.
[11] O. Hardouin Duparc, Le Preston des zones de Guinier–Preston, Cahiers d'histoire de l'aluminium 29 (2001–2002) 57.
[12] G. Fournet, Étude théorique et expérimentale de la diffusion des rayons X par les ensembles denses de particules, PhD thesis, 1951.
[13] C.B. Walter, A. Guinier, An X-ray investigation of age-hardening in Al–Ag, Acta Metall. 1 (1953) 568.
[14] B. Belbeoch, A. Guinier, Relation entre les structures et les propriétés des alliages Al–Ag pendant le durcissement structural, Acta Metall. 3 (1955) 370.
[15] A. Guinier, Théorie et pratique de la radiocristallographie, Dunod, Paris, 1956, nouvelle édition en 1964.
[16] R. Castaing, A. Guinier, Applications à l'analyse métallographique des sondes électroniques, in: Congrès de microscopie électronique de Delft, p. 60 (1949) et de Paris, 1950, p. 391.
[17] A. Guinier, G. Fournet, Small Angle Scattering of X-Rays, J. Willey, New York, 1955.
[18] A. Guinier, La radiocristallographie, Dunod, Paris, 1945.
[19] An adapted version of [15], X-ray diffraction in crystals, imperfect crystals and amorphous body, has been republished in 1994 by Dover Publications, New York
[20] A.-M. Levelut, F. Moussa, J. Doucet, J.-J. Benattar, M. Lambert, B. Dorner, Local order and lattice-dynamics in the ordered phases of TBBA (terephthal-bis-butyl-aniline), J. Phys. 42 (1981) 1651.
[21] A.F. Bonfiglioli, A. Guinier, structure des zones G.P. dans l'alliage Al–Zn au premier stade de leur formation, Acta Metall. 14 (1966) 1213.
[22] (a) M. Lambert, Étude des imperfections de structure du fluorure de lithium irradié, PhD thesis, 1958;
(b) R. Comès, M. Lambert, R. Perret, A. Guinier, Observations des défauts primaires dans les cristaux de fluorure de lithium irradiés par les neutrons thermiques à 77 °K, Phys. Status Solidi B 13 (1966) 265.
[23] (a) A.-M. Levelut, M. Lambert, A. Guinier, Montage permettant l'étude des défauts ponctuels dans les solides par diffusion des rayons X, C. r. hebd. séances Acad. sci. 255 (1962) 319;
(b) A.-M. Levelut, Description d'un montage permettant l'étude des défauts ponctuels par diffusion de rayons X, J. Phys. 24 (1963) 560.
[24] A.-M. Levelut, A. Guinier, Diffusion des rayons X aux petits angles par des substances homogènes, Bull. Soc. Fr. Minéral. Cristallogr. 40 (1967) 445.
[25] E. Dartyge, M. Lambert, G. Leroux, A.-M. Levelut, Étude de l'état de dispersion du soluté dans les solutions solides d'aluminium diluées, Acta Metall. 20 (1972) 233.
[26] M. Lambert, A.-M. Levelut, M. Maurette, H. Heckman, Étude par diffusion des rayons X aux petits angles de mica muscovite irradié par des ions d'argon, Radiat. Eff. 3 (1970) 155.
[27] M. Lambert, A.-M. Levelut, A. Guinier, Étude par diffusion des rayons X aux faibles angles de monocristaux de LiF renfermant des ions Ni^{++} en faible concentration, Acta Crystallogr. A 24 (1968) 549.
[28] E. Dartyge, M. Lambert, Formation de défauts dans les échantillons de mica muscovite irradiés par des ions de grande énergie, Radiat. Eff. 21 (1974) 71.
[29] E. Dartyge, J.P. Duraud, Y. Langevin, M. Maurette, A new method for investigating the past activity of ancient solar flare cosmic rays over a time scale of few billion years, in: Proc. 9th Lunar Planet. Sci. Conf., Houston, TX, 13–17 March, 1978, p. 2375.
[30] M. Lemonnier, D. Petermann, D. Lefur, S. Megtert, Centre national de la recherche scientifique, France, Patent No. 8203344.
[31] P.A. Albouy, J.-P. Pouget, H. Strzelecka, X-ray study of the order-disorder phase transition in a triiodide chain compound: DIPSϕ4(I$_3$)$_{0.76}$, Phys. Rev. B 35 (1987) 173.
[32] A.-M. Levelut, S. Deudé, S. Megtert, D. Petermann, J. Malthète, Point defects in mesophases: a comparison between dilatometric and small angle X-ray scattering studies, Mol. Cryst. Liq. Cryst. 362 (2001) 5.
[33] R. Comès, M. Lambert, A. Guinier, Désordre linéaire dans les cristaux (cas du silicium, du quartz, et des pérovskites ferroélectriques), Acta Crystallogr. A 26 (1970) 244.
[34] M. Lambert, Etude des ferroélectriques au voisinage de la température de transition, in: Colloque 1965 de l'association française de cristallographie, Bull. Soc. Sci. Bretagne 39 (1964) 93.
[35] (a) R. Comès, M. Lambert, A. Guinier, Désordre de structure dans BaTiO$_3$ et KNbO$_3$, C. r. hebd. séances Acad. sci. 266 (1968) 959;
(b) R. Comès, M. Lambert, A. Guinier, The chain structure of BaTiO$_3$ and KNbO$_3$, Solid State Commun. 6 (1968) 715.
[36] R. Comès, F. Denoyer, M. Lambert, Désordre de structure dans les cristaux de type pérovskite, J. Phys., Colloq. 32 (1971) C5a-195.
[37] R. Comès, G. Shirane, Neutron-scattering analysis of the linear-displacement correlations in KTaO$_3$, Phys. Rev. B 5 (1972) 1886.
[38] R. Comès, M. Lambert, H. Launois, H.R. Zeller, Evidence for a peierls distortion or a Kohn anomaly in one-dimensional conductors of the type K$_2$Pt(CN)$_4$Br$_{0.3}\cdot x$H$_2$O, Phys. Rev. B 8 (1973) 571.
[39] J.-P. Pouget, Low dimensional conductors, Chapter 11, in: J. Baruchel, J.-L. Hodeau, M.S. Lehmann, J.-R. Regnard, C. Schlenker (Eds.), Neutron and Synchrotron Radiations for Condensed Matter Studies, in: Applications to Solid State Physics and Chemistry, vol. II, HERCULES school, Les Éditions de Physique and Springer-Verlag, 1993, p. 245.
[40] J.-P. Pouget, Peierls instability and charge density wave in one-dimension electronic conductors, C. R. Physique 17 (2016) 332.
[41] F. Denoyer, R. Comès, A.F. Garito, A.J. Heeger, X-ray-diffuse-scattering evidence for a phase transition in tetrathiafulvalene-tetracyanoquinodimethane (TTF-TCNQ), Phys. Rev. Lett. 35 (1975) 445.
[42] S. Kagoshima, H. Anzai, K. Kajimura, T. Ishiguro, Observation of the Kohn anomaly and the Peierls transition in TTF-TCNQ by X-ray scattering, J. Phys. Soc. Jpn. 39 (1975) 1143.
[43] (a) J.-P. Pouget, S.K. Khanna, F. Denoyer, R. Comès, A.F. Garito, A.J. Heeger, X. Ray, Observation of 2k_{F} and 4k_{F} scatterings in tetrathiafulvalene-tetracyanoquinodimethane (TTF-TCNQ), Phys. Rev. Lett. 37 (1976) 437;
(b) S.K. Khanna, J.-P. Pouget, R. Comès, A.F Garito, A.J. Heeger, X. Ray, Studies of 2k_{F} and 4k_{F} anomalies in TTF-TCNQ, Phys. Rev. B 16 (1977) 1468.
[44] S. Megtert, J.-P. Pouget, R. Comès, Effets structuraux de la dimensionalité dans les conducteurs unidimensionnels, J. Phys., Colloq. 38 (1977) C7-243.
[45] S. Megtert, J.-P. Pouget, R. Comès, X-ray scattering studies from 1D conductors, Ann. N.Y. Acad. Sci. 313 (1978) 234.
[46] J.-P. Pouget, S. Kagoshima, C. Schlenker, J. Marcus, Evidence for a peierls transition in the blue bronzes K$_{0.3}$MoO$_3$ and Rb$_{0.3}$MoO$_3$, J. Phys. Lett., Paris 44 (1983) L113.
[47] S. Fagot, P. Foury-Leylekian, S. Ravy, J.-P. Pouget, H. Berger, One dimensional instability in BaVS$_3$, Phys. Rev. Lett. 90 (2003) 196401.
[48] J.-P. Pouget, S. Ravy, Structural aspects of the Bechgaard salts and related compounds, J. Phys. I 6 (1996) 1501.
[49] M.H. Whangbo, E. Canadell, P. Foury, J.-P. Pouget, Hidden nesting and charge density wave instability in low dimensional metals, Science 252 (1991) 96.
[50] S. Megtert, R. Comès, C. Vettier, R. Pynn, A.F. Garito, Neutron scattering study of commensurability effects in TTF–TCNQ under high pressure, Mol. Cryst. Liq. Cryst. 85 (1982) 159.
[51] F. Dénoyer, R. Currat, Modulated phases in thiourea, in: R. Blinc, A.P. Levanyuk (Eds.), Incommensurate Phases in Dielectrics 2, in: Modern Problems in Condensed Matter Sciences, vol. 14, Elsevier, 1986, p. 129, chapter 14.

[52] D. Durand, F. Dénoyer, R. Currat, M. Lambert, Incommensurate phase in $NaNO_2$, in: R. Blinc, A.P. Levanyuk (Eds.), Incommensurate Phases in Dielectrics 2, in: Modern Problems in Condensed Matter Sciences, vol. 14, Elsevier, 1986, p. 101, chapter 13.

[53] P. Robin, J.-P. Pouget, R. Comès, A. Moradpour, Étude par diffusion des rayons X du mécanisme de polymérisation et des transitions de phase du diacétylène : bis-(*p*-toluène sulfonate) de 2,4 hexadiyne 1,6 diol, J. Phys. 41 (1980) 415.

[54] C.K. Johnson, C.R. Watson, Superstructure and modulation wave analysis for the unidimensional conductor hepta-(tetrathiafulvalene) pentaiodide, J. Chem. Phys. 64 (1976) 2271.

[55] (a) J.M. Hastings, J.-P. Pouget, G. Shirane, A.J. Heeger, N.D. Miro, A.G. Mac Diarmid, Phase-ordering, phase transition and one-dimensional phonons in $Hg_{3-\delta}AsF_6$, Phys. Rev. Lett. 39 (1977) 1484;
(b) J.-P. Pouget, G. Shirane, J.M. Hastings, A.J. Heeger, N.D. Miro, A.G. Mac Diarmid, Elastic neutron scattering of the "phase ordering" phase transition in $Hg_{3-\delta}AsF_6$, Phys. Rev. B 18 (1978) 3645.

[56] S. Megtert, J.-P. Pouget, R. Comès, R. Fourme, X-ray diffuse scattering study of iodine chains in $(TTT)_2I_{3+\delta}$, Lect. Notes Phys. 96 (1979) 196.

[57] (a) H. Endres, J.-P. Pouget, X-ray investigations of compounds containing disordered polyiodide chains, Chem. Scr. 17 (1981) 137 (extended abstract);
(b) H. Endres, J.-P. Pouget, R. Comès, Diffuse X-ray scattering and order-disorder effects in the iodide chain compounds N,N'-diethyl-N,N'-dihydrophenazinium iodide, E2PI1.6, and N,N'-diebenzyl-N,N'-dihydrophenazinium iodide, $B_2PI_{1.6}$, $B_2PI_{1.6}$, J. Phys. Chem. Solids 43 (1982) 739.

[58] P.A. Albouy, J.-P. Pouget, J. Halin, V. Enkelmann, G. Wegner, Structural study of the aging and thermal evolution of polyiodide chains in doped transpolyacetylene, Makromol. Chem. 193 (1992) 853.

[59] C. Bousige, S. Rols, E. Paineau, S. Rouzière, C. Mocuta, B. Verberck, J.P. Wright, H. Kataura, P. Launois, Progressive melting in confined one-dimensional C_{60} chains, Phys. Rev. B 86 (2012) 045446.

[60] F. Rousseaux, R. Moret, D. Guerard, P. Lagrange, M. Lelaurain, Low temperature ordering and phase transitions in KC_{24} and RbC_{24} single crystals, Synth. Met. 12 (1985) 45.

[61] S. Ravy, P.A. Albouy, S. Megtert, R. Moret, J.-P. Pouget, R. Comès, X-ray diffuse scattering from incommensurable structures, Phase Transit. 16 (1989) 193.

[62] R.P. Scaringe, R. Comès, X-ray diffuse scattering, chapter 7, in: Determination of Structural Features of Crystalline and Amorphous Solids, in: Physical Methods of Chemistry, vol. 5, John Wiley, New York, 1990, p. 517.

[63] M. Lambert, Diffuse scattering, Chapter 9, in: J. Baruchel, J.-L. Hodeau, M.S. Lehmann, J.-R. Regnard, C. Schlenker (Eds.), Neutron and Synchrotron Radiations for Condensed Matter Studies, in: Theory, Instruments and Methods, vol. I, HERCULES school, Les Éditions de Physique and Springer-Verlag, 1993, p. 223.

[64] T.R. Welberry, B.D. Butler, Diffuse X-ray scattering from disordered crystals, Chem. Rev. 95 (1995) 2369.

[65] S. Ravy, Study of molecular conductors by X-ray diffuse scattering, Chem. Rev. 104 (2004) 5609.

[66] S. Ravy, P. Launois, R. Moret, J.-P. Pouget, Case studies of molecular disorder, Z. Kristallogr. 220 (2005) 1059.

[67] P. Launois, S. Ravy, R. Moret, Interactions and molecular orientations in solid C_{60}, Int. J. Mod. Phys. B 13 (1999) 253.

[68] S. Ravy, J.-P. Pouget, R. Comès, Destructive interferences between diffuse scatterings due to disorder and displacive modulation (X-ray, white line effect), J. Phys. I 2 (1992) 1173.

[69] A. Guinier, L'effet de la distortion du réseau sur la diffusion des rayons X par un cristal de solution solide, Bull. Soc. Fr. Minéral. Cristallogr. LXXVII (1954) 680.

[70] S. Ravy, From Guinier Preston zones to Friedel oscillations, J. Phys. IV (Proc.) 12 (2002) 7.

[71] (a) S. Rouzière, S. Ravy, J.-P. Pouget, S. Brazovskii, Friedel oscillations and charge-density wave pinning in quasi-one-dimensional conductors: an X-ray diffraction study, Phys. Rev. B 62 (2000), 16231(R);
(b) S. Ravy, S. Rouzière, J.-P. Pouget, J. Marcus, S. Brazovskii, J.F. Berar, E. Elkaim, Disorder effects on the charge-density wave structure in V- and W-doped blue bronzes: Friedel oscillations and charge-density wave pinning, Phys. Rev. B 74 (2006) 174102.

[72] P. Duwez, Structure and properties of glassy metals, Annu. Rev. Mater. Sci. 6 (1976) 83.

[73] J. Dixmier, A. Guinier, Obtention de phases nouvelles par trempe ultra-rapide, Rev. Métall. 64 (1967) 53.

[74] J. Bletry, J.-F. Sadoc, Determination of three partial interference functions of an amorphous Co-P ferromagnet by polarized neutron scattering, J. Phys. F, Met. Phys. 5 (1975) L110.

[75] J.-F. Sadoc, J. Dixmier, A. Guinier, Theoretical calculation of dense random packing of equal and non-equal hard spheres, J. Non-Cryst. Solids 12 (1973) 48.

[76] J.-F. Sadoc, Calcul de la densité maximale d'un empilement aléatoire de sphères dures identiques, C. R. Acad. Sci. Paris, Ser. II 292 (1981) 435.

[77] J. Finney, Fine structure in randomly packed, dense clusters of hard spheres, Mater. Sci. Eng. 23 (1975) 199.

[78] J.-F. Sadoc, Use of regular polytopes for the mathematical description of the order in amorphous structures, J. Non-Cryst. Solids 44 (1981) 1.

[79] D. Shechtman, I. Blech, D. Gratias, J.W. Cahn, Metallic phase with long-range orientational order and no translational symmetry, Phys. Rev. Lett. 53 (1984) 1951.

[80] F. Dénoyer, Diffraction experiments on quasicrystals and related phases, course No. 2, in: F. Axel, et al. (Eds.), From Quasicrystals to More Complex Systems, in: Centre de Physique des Houches Book Series (LHWINTER), vol. 13, Springer Verlag, France, 2000, p. 23.

[81] J. Friedel, F. Dénoyer, Les quasi-cristaux comme alliages de Hume–Rothery, C. R. Acad. Sci. Paris, Ser. II 305 (1987) 171.

[82] S. Haijw, B. Pansu, J.-F. Sadoc, Evidence for a C14 Frank–Kasper phase in one-size gold nanoparticle super lattices, ACS Nano 9 (2015) 8116.

[83] V. Luzatti, X-ray diffraction studies of lipid-water systems, in: D. Chapman (Ed.), Biological Membranes, vol. 1, Academic Press, London, New York, 1968, pp. 71–123.

[84] J. Doucet, A.-M. Levelut, M. Lambert, Long and short-range order in crystalline and smectic B phases of terephthal-bis-butylaniline (TBBA), Mol. Cryst. Liq. Cryst. 24 (1973) 317.

[85] P.S. Pershan, Scattering from Mesomorphic Structures in International Tables for Crystallography, Vol. B, Sect 4.4, third edition, Reciprocal Space, 2008, p. 447.

[86] P. Delord, G. Malet, Diffusion des rayons X par une phase nématique orientée. L'ordre à courte distance dans la *para*-azoxyanisole, Mol. Cryst. Liq. Cryst. 28 (1974) 223.

[87] F. Hardouin, A.-M. Levelut, M.-F. Achard, G. Sigaud, Polymorphisme de substances mésogènes à molécules polaires, J. Chim. Phys. 80 (1983) 53.

[88] A.-M. Levelut, Vacancy-interstitial pairs in ordered smectic phases: a linear Guinier–Preston zone behaviour, J. Phys. 51 (1990) 1517.

[89] R.E. Franklin, R.G. Gosling, Molecular configuration in sodium thymonucleate, Nature 171 (1953) 740.

[90] F. Livolant, A.-M. Levelut, J. Doucet, J.-P. Benoît, The highly concentrated liquid-crystalline phase of DNA is columnar hexagonal, Nature 639 (1989) 724.

[91] J. Doucet, J.-P. Benoit, W.B.T. Cruse, T. Prange, O. Kennard, Coexistence of A- and B- form DNA in a single crystal lattice, Nature 337 (1989) 190.

[92] A.-M. Levelut, Structure of a disk-like mesophase, J. Phys. Lett. 40 (1979) L81.

[93] J. Malthête, A.M. Levelut, Mesophase formed by diabolo-like molecules, Adv. Mater. 3 (1991) 94.

[94] J. Malthète, A.-M. Levelut, L. Liebert, The mesomorphism of some diamides of alkyl-substituted-1, 3-diaminobenzene, Adv. Mater. 4 (1992) 37.

[95] P.-A. Albouy, D. Guillon, B. Henrich, A.-M. Levelut, J. Malthète, Structural study of the nematic and hexagonal columnar phases of wired shaped self assemblies of thermotropic mesogens, J. Phys. II 5 (1995) 1617.

[96] J. Charvolin, P. Manneville, B. Deloche, Magnetic resonance of perdeuterated potassium laurate in oriented soap-water multilayers, Chem. Phys. Lett. 23 (1973) 345.
[97] P. Davidson, P. Keller, A.-M. Levelut, Molecular organization in side chain liquid crystalline polymers, J. Phys. 46 (1985) 939.
[98] P. Davidson, A.-M. Levelut, Evidence by X-ray scattering of defects in the lamellar stacking of the SmA phase of a side-chain polymer, J. Phys. 49 (1988) 689.
[99] A.-M. Levelut, Structure of liquid crystals, Chapter 5, in: J. Baruchel, J.L. Hodeau, M.S. Lehmann, J.-R. Regnard, C. Schlenker (Eds.), Neutron and Synchrotron Radiations for Condensed Matter Studies, in: Applications to Soft Condensed Matter and Biology, vol. III, HERCULES school, Les Éditions de Physique and Springer-Verlag, 1994, p. 69.
[100] A.-M. Levelut, Structure des phases mésomorphes formées de molécules discoïdes, J. Chim. Phys. 80 (1983) 149.
[101] (a) J. Doucet, J.-P. Benoit, Molecular dynamics studied by analysis of the X-ray diffuse scattering from lysozyme crystals, Nature 325 (1987) 643;
(b) J. Doucet, J.-P. Benoit, P. Faure, D. Durand, Analyse de la diffusion diffuse donnée par les cristaux de protéine, J. Phys. I 2 (1992) 981.
[102] (a) P. Davidson, J.C.P. Gabriel, Mineral liquid crystals, Curr. Opin. Colloid Interface Sci. 9 (2005) 377;
(b) P. Davidson, J.C.P. Gabriel, Orientational order in clay gels, Clay Sci. 12 (Suppl. 1) (2005) 21.
[103] A. Guinier, As chance would have it..., Rigaku J. 16 (1999) 2.
[104] S. Fagot, P. Foury-Leylekian, S. Ravy, J.-P. Pouget, M. Anne, G. Popov, M.V. Lobanov, M. Greenblatt, Structural aspects of the metal-insulator phase transition of $BaVS_3$, Solid State Sci. 7 (2005) 718.
[105] G. Monet, M.S. Amara, S. Rouzière, E. Paineau, Z. Chai, J.D. Elliott, E. Poli, M.-L. Liu, G. Teobaldi, P. Launois, Structural resolution of inorganic nanotubes with complex stoichiometry, Nat. Commun. 9 (2018) 2033.
[106] P. Davidson, C. Penisson, D. Constantin, J.C.P. Gabriel, Isotropic, nematic, and lamellar phases in colloidal suspensions of nanosheets, Proc. Natl. Acad. Sci. USA 115 (2018) 201802692.
[107] S. Ravy, J.-P. Itié, A. Polian, M. Hanfland, High-pressure study of X-ray diffuse scattering in ferroelectric perovskites, Phys. Rev. Lett. 99 (2007) 117601.
[108] P. Mach, R. Pindak, A.-M. Levelut, P. Barois, H.T. Nguyen, C.C. Huang, L. Furenlid, Structural characterization of various chiral smectic C phases by resonant X-ray scattering, Phys. Rev. Lett. 81 (1998) 1015.
[109] S. Fagot, P. Foury-Leylekian, S. Ravy, J.-P. Pouget, E. Lorenzo, Y. Joly, M. Green blatt, M.V. lobanov, G. Popov, X-ray anomalous scattering investigation of $BaVS_3$, Phys. Rev. B 73 (2006) 033102.
[110] P. Leininger, V. Ilakovac, Y. Joly, E. Schierle, E. Weschke, O. Buneau, H. Berger, J.-P. Pouget, P. Foury-Leylekian, Ground state of the quasi-1D $BaVS_3$ resolved by resonant magnetic X-ray scattering, Phys. Rev. Lett. 106 (2011) 167203.
[111] D. Le Bolloc'h, S. Ravy, J. Dumas, J. Marcus, F. Livet, C. Detlefs, F. Yakhou, L. Paolasini, Charge density wave dislocation as revealed by coherent X-ray diffraction, Phys. Rev. Lett. 95 (2005) 116401.
[112] C. Laulhé, T. Huber, G. Lantz, A. Ferrer, S.O. Mariager, S. Grübel, J. Rittmann, J.A. Johnson, V. Esposito, A. Lübcke, L. Huber, M. Kubli, M. Savoini, V.L.R. Jacques, L. Cario, B. Corraze, E. Janod, G. Ingold, P. Beaud, S.L. Johnson, S. Ravy, Ultrafast formation of a charge density wave state in 1T-TaS_2: observation at nanometer scales using time-resolved X-ray diffraction, Phys. Rev. Lett. 118 (2017) 247401.
[113] A. Guinier, Les rayons X, Collection Que sais-je?, Presses universitaires de France, 1984.
[114] A. Guinier, La structure de la matière : Du ciel bleu aux cristaux liquides, Préface de A. Kastler, Collection Liaisons Scientifiques, Hachette et CNRS, 1980 ;
The Structure of Matter: From Blue Sky to Liquid Crystals, Hodder Arnold, 1984.
[115] A. Guinier, R. Julien, La matière à l'état solide : Des supraconducteurs aux superalliages, Préface de Sir Nevill Mott, Collection, Liaisons scientifiques, Hachette et CNRS, 1987 ;
The Solid State: From Superconductors to Superalloys, International Union of Crystallography, Texts on Crystallography Series, vol. 1, Oxford University Press, 1989.